

1                    Harnessing Large Language Models for Adaptive and  
2                    Explainable Traffic Forecasting

3                    Haoyang Yan<sup>1</sup> and Xiaolei Ma<sup>\*1,2</sup>

4                    <sup>1</sup>School of Transportation Science and Engineering, Beihang University, Beijing,  
5                    China.

6                    <sup>2</sup>Key Laboratory of Intelligent Transportation Technology and System of the  
7                    Ministry of Education, Beihang University, Beijing 102206, China

8                    \*Address correspondence to: xiaolei@buaa.edu.cn

9                    **Abstract**

10                  Accurate traffic state prediction is a cornerstone of Intelligent Transportation Systems (ITS).  
11                  While deep learning models—specifically Graph Neural Networks (GNNs) and Transformers—  
12                  have achieved state-of-the-art performance in routine forecasting, they exhibit significant fragility  
13                  under anomalous conditions (e.g., accidents, extreme weather, public events) due to their re-  
14                  liability on historical stationarity. Furthermore, the “black-box” nature of these models precludes  
15                  interpretability, limiting their operational utility. To address these deficiencies, this study  
16                  proposes Chat-ITS, a novel hybrid framework that synergizes robust probabilistic time-series  
17                  forecasting with the semantic reasoning capabilities of Large Language Models (LLMs). The  
18                  methodology comprises three mathematically formalized stages: (1) A foundation model based  
19                  on discrete tokenization and sequence-to-sequence learning generates a probabilistic distribu-  
20                  tion of future trajectories; (2) A cross-modal reasoning module, driven by an LLM, processes  
21                  heterogeneous unstructured text data to perform Bayesian-like contextual adjustments on the  
22                  candidate trajectories; (3) An operational interface generates explainable diagnostics and action-  
23                  able control strategies. Extensive experiments on large-scale real-world datasets from Beijing  
24                  demonstrate that Chat-ITS reduces prediction error by up to 15% during non-recurring con-  
25                  gestion events compared to baselines, while offering zero-shot generalization to unseen event  
26                  types.

27                  **1 Introduction**

28                  Accurate traffic prediction is fundamental to the efficacy of Intelligent Transportation Systems  
29                  (ITS), enabling critical functions such as dynamic route guidance, adaptive traffic signal control,  
30                  and proactive incident management essential for mitigating congestion, reducing emissions, and  
31                  enhancing urban mobility resilience [1]. Congestion alone costs economies billions annually and

32 degrades quality of life in urban centers [2]. Effective ITS, powered by reliable forecasts, promises  
33 substantial improvements in transportation efficiency and sustainability. Recent advances, partic-  
34 ularly the application of deep learning techniques like graph neural networks (GNNs) for modeling  
35 complex spatial dependencies across road networks [3] and sophisticated sequence models (e.g., tem-  
36 poral convolution networks, attention mechanisms) for capturing temporal dynamics [4, 5], have  
37 considerable improved short-term forecasting accuracy under typical, recurring traffic conditions [6].  
38 These methods effectively learn patterns from large historical datasets, providing a strong foundation  
39 for next-generation ITS applications operating under predictable circumstances.

40 Despite these successes, existing state-of-the-art traffic forecasting methods face critical limita-  
41 tions that hinder their real-world operational utility, particularly under non-routine circumstanc-  
42 es [7–9]. Firstly, their predictive performance often degrades sharply during anomalous events such as  
43 road accidents, unexpected road closures, severe weather conditions, or large-scale public gatherings  
44 [10, 11]. Models trained primarily on routine historical patterns often exhibit poor generalization  
45 capabilities when faced with data distributions shifted by these irregular occurrences [12, 13]. This  
46 fragility undermines their reliability precisely when accurate prediction is most needed for effective  
47 incident response and management. Secondly, the fixed input encoding mechanisms of many deep  
48 learning models limit their ability to flexibly incorporate diverse, unstructured, or dynamic updates  
49 on road work schedules often contains crucial context for anticipating traffic impacts. Integrating  
50 textual incident reports, event schedules, social media alerts, or unforeseen disruptions often requires  
51 complex feature engineering or extensive model retraining, impeding adaptation to unforeseen event  
52 types without clear overhead [14]. Thirdly, and perhaps most crucially for translation into practice,  
53 the standard output of these models, typically a high-dimensional matrix or tensor representing  
54 predicted speeds or flows, lacks direct interpretability. It fails to convey the underlying reasons for  
55 the predicted state or provide actionable guidance for traffic operators and decision-makers [15].  
56 Consequently, even statistically accurate forecasts may not readily translate into effective, timely,  
57 and context-aware traffic management interventions, limiting the practical impact of these advanced  
58 techniques.

59 Large language models (LLMs) have emerged as powerful tools demonstrating remarkable ca-  
60 pabilities in natural language understanding, contextual reasoning, and generalization across di-  
61 verse tasks [16]. Their potential to process unstructured text, synthesize information from multiple  
62 sources, and generate human-like explanations offers promising avenues to address the challenges of  
63 context integration and interpretability in ITS [7, 17, 18]. However, applying LLMs directly to the  
64 task of numerical time-series forecasting presents inherent difficulties. Their architectures, primar-  
65 ily optimized for sequential token generation, often struggle with the precise numerical regression  
66 required for traffic state prediction and can be inefficient in capturing the complex spatio-temporal  
67 statistical dependencies inherent in traffic flow [14, 19]. Furthermore, training or even fine-tuning  
68 large LLMs for specialized forecasting tasks demands substantial computational resources and large-  
69 scale, domain-specific datasets, often proving impractical for widespread deployment in operational  
70 ITS settings where data characteristics can vary across locations and time [20].

71 Here, we introduce Chat-ITS, a novel hybrid forecasting framework designed to bridge the gap be-  
72 tween robust probabilistic time-series modeling and the contextual reasoning capabilities of LLMs,

73 thereby overcoming the aforementioned limitations. Chat-ITS employs a synergistic, multi-stage  
74 approach that deliberately leverages the distinct strengths of each component. It first utilizes a  
75 dedicated spatio-temporal foundation model, pre-trained on extensive historical traffic data, to gen-  
76 erate multiple candidate traffic state trajectories along with associated uncertainty estimates. This  
77 ensures statistical rigor and captures complex baseline traffic dynamics. Subsequently, an LLM, op-  
78 erating on these candidate trajectories, is conditioned on flexible natural language prompts. These  
79 prompts can seamlessly encode both structured data (e.g., quantitative weather forecasts, road clo-  
80 sure notices with coordinates and times) and unstructured descriptions rich with linguistic cues (e.g.,  
81 "Event update: sold-out show at the downtown arena, scheduled to end at 10 PM" or "Dispatch  
82 log: report of a multi-vehicle collision with emergency services responding on the northbound lane  
83 near exit 15"). The LLM evaluates the candidate trajectories within this broader context, reasoning  
84 about the likely impacts to select or adjust towards the most plausible outcome given the real-time  
85 information. Crucially, the LLM also generates human-readable explanations for its choice and  
86 actionable recommendations tailored for traffic management personnel, integrating insights poten-  
87 tially learned from historical operational data. This architecture deliberately avoids tasking the  
88 LLM with direct numerical prediction, instead harnessing its strengths in semantic comprehension,  
89 causal inference, and context-aware reasoning.

90 We demonstrate through comprehensive experiments encompassing both routine traffic patterns  
91 and a diverse set of simulated and real-world anomalous scenarios (including construction, accidents,  
92 and public events) that Chat-ITS noticeably outperforms conventional deep learning baseline mod-  
93 els during irregular events, reducing prediction errors by up to 15% under certain conditions, while  
94 matching state-of-the-art accuracy under normal conditions. Crucially, case studies highlight the  
95 framework's ability to generalize zero-shot to unseen event types described only via text prompts  
96 and deliver context-aware, actionable insights (e.g., suggesting specific signal timing adjustments,  
97 disseminating targeted traveler advisories, or recommending dynamic routing strategies). By in-  
98 tegrating the statistical power of probabilistic forecasting with the semantic understanding and  
99 reasoning capabilities of language-based AI, Chat-ITS presents a new paradigm for traffic predic-  
100 tion, one that is not only accurate and adaptive but also explainable and directly aligned with the  
101 practical needs of transportation practitioners for effective real-world ITS deployment.

## 102 **2 Literature Review**

### 103 **2.1 Deep Learning for Traffic Forecasting**

104 Traffic forecasting has evolved from traditional statistical and regression-based approaches to deep  
105 learning models capable of capturing complex temporal dynamics. Early studies primarily relied on  
106 Recurrent Neural Networks (RNNs), particularly Long Short-Term Memory (LSTM) architectures,  
107 to model sequential dependencies in traffic speed and flow data [21, 22]. While effective in temporal  
108 modeling, these approaches are limited in their ability to explicitly represent the non-Euclidean  
109 spatial topology of road networks.

110 To address this limitation, Spatio-Temporal Graph Neural Networks (STGNNs) have been widely

111 adopted. Representative models such as DCRNN and Graph WaveNet combine graph convolutions  
112 with temporal sequence modeling to capture spatial correlations and temporal dynamics simulta-  
113 neously [23, 24]. Subsequent works have extended these frameworks by relaxing the assumption of  
114 static spatial dependencies. For instance, Traffic Transformer introduces global-local decoders to  
115 hierarchically aggregate spatial features [25], while PDFormer incorporates propagation delay-aware  
116 attention to explicitly model temporal lags in traffic interactions [26].

117 Despite their expressive power, the necessity of graph convolution has recently been questioned.  
118 Empirical studies indicate that simplified spatial modeling strategies can achieve comparable per-  
119 formance with substantially reduced computational overhead. SimST demonstrates that lightweight  
120 spatial aggregation approximates the effectiveness of GCN-based methods [27]. Similarly, MLP-  
121 based architectures such as ST-MLP [28] and STID [29] show that concise spatio-temporal identity  
122 mappings can outperform complex GNNs by reducing overfitting to noisy spatial correlations.

123 In parallel, Transformer-based models have gained attention for their ability to capture long-  
124 range temporal dependencies. PatchTST segments time series into patches to preserve local temporal  
125 semantics [30], whereas iTransformer inverts the attention mechanism to better model multivariate  
126 correlations [31]. To further account for uncertainty and stochasticity in traffic systems, probabilistic  
127 generative approaches such as SpecSTG [32] and Diffusion-TS [15] have been proposed, enabling  
128 uncertainty-aware forecasting and data imputation.

## 129 2.2 Foundation Models for Time Series

130 Inspired by the “pre-train and fine-tune” paradigm in Natural Language Processing, recent research  
131 has shifted toward the development of foundation models for time series analysis [33, 34]. These  
132 models aim to learn universal temporal representations that generalize across datasets and tasks,  
133 enabling zero-shot or few-shot inference.

134 Chronos adapts T5-style architectures by discretizing continuous values into token sequences,  
135 achieving strong zero-shot performance across diverse domains [35]. Lag-Llama adopts a probabilis-  
136 tic modeling framework to capture scaling behaviors over large-scale time-series corpora [36]. To  
137 model multi-periodicity, TimesNet reformulates one-dimensional time series into two-dimensional  
138 representations, facilitating variation modeling via convolutional kernels [37].

139 Recent efforts further emphasize unified modeling across heterogeneous tasks. UniTS proposes  
140 a prompt-based backbone capable of jointly addressing forecasting, classification, and imputation  
141 [38], while Moirai-MoE introduces a Mixture-of-Experts architecture to handle diverse temporal res-  
142 olutions without manual frequency alignment [39]. Another research direction explores the reuse of  
143 frozen pre-trained language or vision models. One Fits All demonstrates that large language models  
144 can be adapted to time series with minimal parameter updates [40]. Nevertheless, most existing  
145 foundation models operate exclusively on numerical signals, limiting their ability to incorporate un-  
146 structured contextual information, such as event descriptions, that is often critical for interpreting  
147 anomalies in intelligent transportation systems [41].

148 **2.3 Large Language Models in Transportation**

149 The application of Large Language Models (LLMs) in transportation research introduces a paradigm  
150 shift from purely numerical modeling toward semantic reasoning and agent-based decision making.  
151 A central challenge lies in aligning continuous time series data with the discrete token-based rep-  
152 resentations of LLMs. Time-LLM and LLM4TS address this issue through reprogramming and  
153 fine-tuning strategies that encode numerical sequences as language tokens [20, 42].

154 In urban computing scenarios, UrbanGPT integrates spatio-temporal dependency encoders with  
155 instruction tuning to improve generalization under data scarcity [43], while ST-LLM reformulates  
156 spatio-temporal observations as token sequences to capture global network dependencies [44]. Be-  
157 yond forecasting, LLMs have been explored for explanation, simulation, and decision support. TF-  
158 LLM and ChatTraffic generate natural language interpretations of traffic conditions and congestion  
159 causes, enhancing model interpretability [45, 46]. CityGPT further extends this idea by constructing  
160 a city-scale world model in which LLM-based agents perform diverse urban tasks [18].

161 More advanced frameworks adopt “LLM-in-the-loop” architectures. TimeCAP and TimeXL  
162 employ multi-agent systems in which LLMs generate contextual summaries or reasoning paths that  
163 guide downstream numerical predictors [47, 48]. Additionally, external information sources such as  
164 social events and news reports have been incorporated via generative agents to stabilize forecasting  
165 under non-stationary conditions [49]. Nevertheless, a fundamental challenge remains in effectively  
166 reconciling the numerical accuracy of specialized time-series models with the high-level semantic  
167 reasoning capabilities of LLMs, particularly for real-time anomaly detection and intervention.

168 **3 Preliminary**

169 Traffic prediction is typically framed as a short-term time-series forecasting task, where future values  
170  $\mathbf{X}_{T+1:T+n}$  are predicted based on historical observations  $\mathbf{X}_{1:T}$ . This paper tackles a multi-modal  
171 version of this problem, recognizing that real-world traffic dynamics are influenced not only by  
172 past traffic states but also by a plethora of contextual factors often conveyed through textual or  
173 structured non-time-series data. We work with input instances  $(\mathbf{X}_{1:T}, \mathbf{s})$ , consisting of historical  
174 time series data  $\mathbf{X}_{1:T} = \{\mathbf{x}_1, \dots, \mathbf{x}_T\}$ , where each  $\mathbf{x}_t \in \mathbb{R}^N$  captures  $D$  features of traffic states (e.g.,  
175 speed, flow, occupancy) for  $N$  spatial locations (e.g., road segments, sensors) over  $T$  historical time  
176 steps, and auxiliary contextual information  $\mathbf{s}$ . This contextual information  $\mathbf{s}$  can be diverse, including  
177 structured data (e.g., weather parameters, event schedules, road work logs) and unstructured natural  
178 language text (e.g., incident reports, social media alerts, news feeds) that potentially influences the  
179 time series and provides valuable context for improving forecast accuracy, especially during non-  
180 routine conditions. Our objective is to develop a model  $\mathcal{F}$  that takes these multi-modal inputs to accurate  
181 and reliable predictions of future traffic states, potentially including uncertainty quantification. This  
182 is formalized as:

$$\mathbf{X}_{T+1:T+n} = \{\mathbf{x}_{T+1}, \mathbf{x}_{T+2}, \dots, \mathbf{x}_{T+n}\} = \mathcal{F}(\mathbf{X}_{1:T}, \mathbf{s}), \quad (1)$$

183 where  $\mathbf{X}_{T+1:T+n}$  is the predicted sequence of  $n$  future state vectors or distributions. The ultimate  
184 goal is to identify an optimal model  $\mathcal{F}$  that delivers accurate and reliable predictions while also being

185 explainable and effectively leveraging the contextual information from  $\mathbf{s}$  to adapt to both routine  
 186 and non-routine conditions.

## 187 4 Methodology

### 188 4.1 Overall Framework

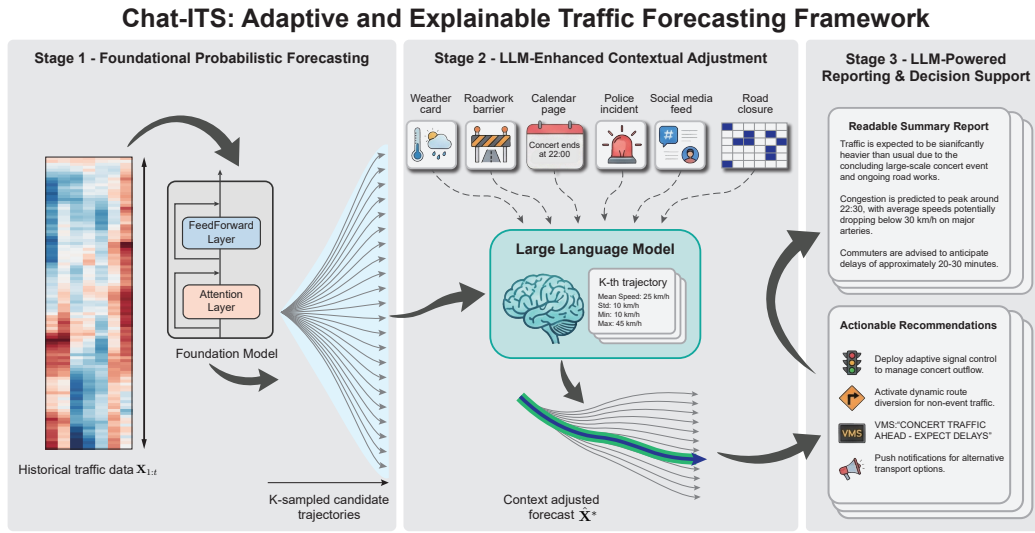


Figure 1: Overall architecture of the Chat-ITS framework. (A) Stage 1: A pre-trained spatio-temporal foundation model processes historical traffic data  $\mathbf{X}_{1:T}$  to generate multiple candidate future trajectories  $\{\hat{\mathbf{X}}^{(k)}\}$  representing a baseline probabilistic forecast. (B) Stage 2: Real-time contextual information  $\mathbf{s}$ , including structured and unstructured event data, is processed by an LLM. The LLM reasons about the event's impact and evaluates the candidate trajectories, selecting or adjusting to the most plausible event-conditioned forecast  $\hat{\mathbf{X}}^*$ . (C) Stage 3: The adjusted forecast, along with historical dispatch patterns, feeds into the LLM to generate human-readable summary reports and actionable traffic management recommendations.

189 The Chat-ITS framework, depicted schematically in Fig.1, operates through three synergistic  
 190 core stages designed to integrate the strengths of advanced time-series modeling and large language  
 191 models: (1) Foundational Probabilistic Forecasting, (2) LLM-Enhanced Contextual Adjustment,  
 192 and (3) LLM-Powered Reporting and Decision Support.

- 193 • **Stage 1: Foundational Probabilistic Forecasting (Fig.1 A):** The foundation of Chat-  
 194 ITS is a robust forecasting model capable of capturing complex dependencies in traffic data  
 195 and providing probabilistic outputs. We employ a state-of-the-art architecture pre-trained  
 196 on extensive historical traffic data. To ensure the model learns representative patterns, the  
 197 pre-training data include curated subsets, such as: (i) time-series from high-volume road seg-  
 198 ments or grid cells representing typical urban traffic dynamics, and (ii) traffic data aggregated  
 199 around key venues (stadiums, transport hubs, event centers) known to generate non-standard  
 200 patterns. Inspired by architectures like Chronos [35] which adapt language transformer-based

201 models for time-series, our foundation model processes the historical input and generates not a  
 202 single prediction, but multiple trajectory samples  $\{\hat{\mathbf{X}}_{T+1:T+n}^{(k)}\}_{k=1}^K$ . These samples collectively  
 203 approximate the predictive distribution  $P(\mathbf{X}_{T+1:T+n}|\mathbf{X}_{1:T})$ , providing a baseline probabilistic  
 204 forecast and inherent uncertainty quantification, crucial for representing the range of possibil-  
 205 ities under routine conditions.

- 206 • **Stage 2: LLM-Enhanced Contextual Adjustment (Fig.1 B):** This stage integrates  
 207 real-time contextual information  $\mathbf{s}$  to refine the baseline forecast, addressing the limitations of  
 208 models relying solely on historical patterns. The contextual information  $\mathbf{s}$ , which can include  
 209 structured data and unstructured text, is processed by an LLM. The LLM executes a chain-of-  
 210 thought process: first summarizing the event information, then reasoning about its likely causal  
 211 impact on traffic flow (location, severity, duration), and finally assessing the quantitative effect.  
 212 Then the LLM selects the most plausible trajectory  $\hat{\mathbf{X}}_{T+1:T+n}^*$  or potentially generates an  
 213 adjusted trajectory that better reflects the anticipated impact of the event. This step leverages  
 214 the LLM’s ability to understand and reason about novel or complex situations described in  
 215 natural language, effectively modulating the initial probabilistic forecast based on real-time  
 216 context.
- 217 • **Stage 3: LLM-Powered Reporting and Decision Support (Fig.1 C):** The final stage  
 218 focuses on translating the adjusted forecast  $\hat{\mathbf{X}}_{T+1:T+n}^*$  into practical outputs for end-users. The  
 219 LLM receives the context-adjusted forecast and potentially relevant historical traffic guidance  
 220 data. This historical guidance data allows the LLM to learn implicit operational preferences  
 221 and common responses implemented by human traffic controllers in similar past situations.  
 222 Based on the adjusted forecast, the contextual information, and the learned operational pat-  
 223 terns, the LLM generates: (i) a concise, human-readable summary report describing the antici-  
 224 pated traffic conditions, highlighting potential issues (e.g., specific bottlenecks, expected delay  
 225 increases), and explaining the reasoning based on the contextual factors; and (ii) actionable  
 226 recommendations for traffic management (e.g., “Consider adjusting signal timing plan B on  
 227 Corridor X between 8-10 AM,” “Disseminate advisory regarding lane closure on Highway Y,”  
 228 “Prepare diversion route Z”). This stage bridges the gap between raw numerical prediction  
 229 and practical operational utility, providing explainable insights and decision support.

## 230 4.2 Stage 1: Foundational Probabilistic Forecasting

231 In this stage, we reformulate the time-series forecasting problem as a specialized language modeling  
 232 task. By mapping continuous traffic dynamics into discrete semantic tokens, we leverage the robust  
 233 reasoning capabilities of the Transformer architecture to capture complex temporal dependencies  
 234 and model the aleatoric uncertainty inherent in stochastic traffic flows.

### 235 4.2.1 Sequence Serialization and Tokenization Strategy

236 Unlike traditional point-wise forecasting models, we adopt a patch-based tokenization strategy in-  
 237 spired by the Chronos paradigm [35]. This approach reduces the sequence length complexity from

238  $O(T^2)$  to  $O((T/S)^2)$  while preserving local temporal semantics.

239 **Temporal Patching** Given a univariate time series  $\mathbf{x}^i = \{x_1^i, \dots, x_T^i\} \in \mathbb{R}^T$  for a spatial node  $i$ ,  
240 we first decompose the sequence into a series of overlapping patches. Let  $P$  denote the patch length  
241 and  $S$  the stride. The sequence is unfolded into a matrix of patches  $\mathcal{P}^i = \{\mathbf{p}_1^i, \dots, \mathbf{p}_N^i\}$ , where the  
242  $j$ -th patch  $\mathbf{p}_j^i \in \mathbb{R}^P$  is defined as:

$$\mathbf{p}_j^i = [x_{(j-1)S+1}^i, \dots, x_{(j-1)S+P}^i] \quad (2)$$

243 where  $N = \lfloor (T - P)/S \rfloor + 1$  is the number of tokens.

244 **Local Scaling for Stationarity** Traffic data exhibits significant non-stationarity (e.g., varying  
245 peak hours across days). To ensure the distribution of values within each patch falls into a learnable  
246 range for the quantizer, we apply instance-level mean scaling. For each patch  $\mathbf{p}_j^i$ , we compute a  
247 local scale factor  $s_j = \frac{1}{P} \sum_{k=1}^P |\mathbf{p}_{j,k}^i| + \epsilon$ . The scaled patch is obtained via:

$$\tilde{\mathbf{p}}_j^i = \frac{\mathbf{p}_j^i}{s_j} \quad (3)$$

248 This normalization allows the model to learn scale-invariant temporal patterns, generalizing across  
249 different traffic volume levels.

250 **Quantization and Vocabulary Mapping** To interface with the categorical nature of language  
251 models, we map the continuous scaled domain  $\mathbb{R}$  to a discrete codebook  $\mathcal{C} = \{c_1, \dots, c_V\}$  of size  $V$ .  
252 We employ a quantization function  $Q : \mathbb{R} \rightarrow \{1, \dots, V\}$  using uniform binning within a fixed range  
253  $[\min, \max]$ . The token ID  $z_{j,k}$  for the  $k$ -th element of the  $j$ -th patch is derived as:

$$z_{j,k} = Q(\tilde{p}_{j,k}^i) = \text{clip}\left(\left\lfloor \frac{\tilde{p}_{j,k}^i - \min}{\max - \min} \times (V - 1) \right\rfloor, 0, V - 1\right) \quad (4)$$

254 Consequently, the continuous time series  $\mathbf{x}^i$  is transformed into a sequence of discrete token IDs  
255  $\mathbf{Z}^i = \{z_{1,1}, \dots, z_{N,P}\}$ , which serves as the “sentence” input to the Transformer.

#### 256 4.2.2 Encoder-Decoder Architecture

257 We employ a modified T5 (Text-to-Text Transfer Transformer) backbone [50] to process the tokenized  
258 traffic sequences. The architecture consists of an encoder that maps the historical token sequence  
259 to a latent representation, and a decoder that autoregressively generates future tokens.

260 **Self-Attention with Relative Position Bias** The core mechanism is the Multi-Head Self-  
261 Attention (MHSA). Unlike standard Transformers that use absolute sinusoidal positional encodings,  
262 T5 utilizes relative positional embeddings, which is crucial for time series as it naturally models the  
263 “time lag” distance between patches. The attention score between query  $q$  and key  $k$  is computed

264 as:

$$\mathcal{A}_{q,k} = \text{softmax} \left( \frac{\mathbf{Q}\mathbf{K}^T}{\sqrt{d_{model}}} + \mathbf{B}_{q,k} \right) \mathbf{V} \quad (5)$$

265 where  $\mathbf{B}_{q,k}$  is a learnable scalar bias added to the attention logit, representing the relative temporal  
266 distance between position  $q$  and  $k$ .

267 **Objective Function** The model is trained to minimize the standard Cross-Entropy loss over the  
268 vocabulary  $V$ . Given the historical context  $\mathbf{Z}_{<t}$ , the model predicts the probability distribution of  
269 the next token  $z_t$ :

$$\mathcal{L}_{\text{CE}} = - \sum_{t=1}^L \log P_\theta(z_t | \mathbf{Z}_{<t}) \quad (6)$$

270 We incorporate a multi-task learning objective by combining the primary forecasting task with a  
271 random masking reconstruction task (BERT-style) to enhance the model's robustness against missing  
272 data and noise.

#### 273 4.2.3 Probabilistic Trajectory Generation

274 To capture the aleatoric uncertainty inherent in future traffic states, we move beyond point estima-  
275 tion to probabilistic trajectory generation.

276 **Nucleus Sampling (Top- $p$ )** During inference, instead of greedy decoding (selecting the token  
277 with max probability), we approximate the posterior distribution  $P(\mathbf{X}_{\text{future}} | \mathbf{X}_{\text{history}})$  by sampling  $K$   
278 independent hypotheses (trajectories). We employ Nucleus Sampling, which truncates the tail of the  
279 distribution, considering only the smallest set of top tokens whose cumulative probability exceeds a  
280 threshold  $p$ :

$$\mathcal{V}^{(p)} = \{z \in \mathcal{C} \mid \sum_{z' \in \mathcal{V}^{(p)}} P_\theta(z' | z_{<t}) \geq p\} \quad (7)$$

281 At each step  $t$ , the next token  $z_t^{(k)}$  for the  $k$ -th hypothesis is sampled from the re-normalized  
282 distribution over  $\mathcal{V}^{(p)}$ .

283 **De-tokenization and Aggregation** The generated token sequences are mapped back to the  
284 continuous domain via inverse quantization and inverse scaling using the stored local scale factors  
285  $s_j$ . Since patches overlap, the value at a specific time step  $t$  is reconstructed by averaging the  
286 predictions from all patches covering that step, ensuring smoothness at patch boundaries:

$$\hat{x}_t^{(k)} = \frac{1}{|\Omega_t|} \sum_{j \in \Omega_t} s_j \cdot Q^{-1}(z_{j,\text{idx}(t)}^{(k)}) \quad (8)$$

287 where  $\Omega_t$  is the set of patches containing time step  $t$ . This process yields a set of candidate trajectories  
288  $\mathcal{H} = \{\hat{\mathbf{X}}^{(1)}, \dots, \hat{\mathbf{X}}^{(K)}\}$  representing plausible future scenarios.

289 **4.3 Stage 2: Logic-Enhanced Contextual Trajectory Selection**

290 While Stage 1 provides a robust probabilistic baseline based on historical patterns, it lacks the se-  
 291 mantic understanding to account for varying external disruptions (e.g., accidents, extreme weather).  
 292 Stage 2 bridges this gap by employing a Large Language Model (LLM) as a logic-driven reasoner to  
 293 evaluate and select the most plausible trajectory  $\hat{\mathbf{X}}^*$  from the candidate set  $\mathcal{H}$  based on real-time  
 294 context  $\mathbf{s}$ .

295 **4.3.1 Semantic Serialization of Probabilistic Forecasts**

296 Since LLMs operate in the semantic space rather than the numerical tensor space, we must project  
 297 the candidate set  $\mathcal{H} = \{\hat{\mathbf{X}}^{(1)}, \dots, \hat{\mathbf{X}}^{(K)}\}$  into a textual representation compatible with the LLM’s  
 298 context window. We define a serialization function  $\psi : \mathbb{R}^n \rightarrow \mathcal{S}$  that aggregates high-dimensional  
 299 trajectory data into descriptive statistics. For each candidate  $k$ , we compute the statistical summary  
 300 vector  $\mathbf{v}^{(k)}$  over key corridors, including the minimum, median, and maximum speeds across the  
 301 prediction horizon. This is formatted into a structured prompt segment:

$$\mathcal{T}_{traj}^{(k)} = \text{"Candidate } k : \text{Trend } \in [\min(\mathbf{v}^{(k)}), \max(\mathbf{v}^{(k)})], \text{Dynamics: Description}(\nabla \mathbf{v}^{(k)})"} \quad (9)$$

302 where  $\text{Description}(\cdot)$  maps numerical gradients to linguistic descriptors (e.g., “rapidly decaying,”  
 303 “stable”). This allows the LLM to comprehend the traffic dynamics implied by each hypothesis  
 304 without processing raw tensors.

305 **4.3.2 Chain-of-Thought Reasoning and Selection**

306 We leverage the reasoning capabilities of the Qwen2.5-14B-Instruct model [51] to model the causal  
 307 relationship between the context  $\mathbf{s}$  and traffic states. The inference process is structured as a  
 308 conditional probability maximization problem via Chain-of-Thought (CoT) prompting.

309 Let  $\mathcal{P}_{sys}$  be the system instruction and  $\mathcal{T}_{ctx}$  be the textualized real-time context (e.g., incident  
 310 logs, weather reports). The LLM generates a reasoning path  $\mathcal{R}$  followed by a selection index  $k^*$ :

$$(\mathcal{R}, k^*) \sim P_{LLM}(\cdot | \mathcal{P}_{sys}, \mathcal{T}_{ctx}, \{\mathcal{T}_{traj}^{(k)}\}_{k=1}^K) \quad (10)$$

311 The reasoning path  $\mathcal{R}$  explicitly decomposes the task into three logical steps:

- 312 1. **Event Impact Analysis:** The LLM parses  $\mathcal{T}_{ctx}$  to extract event attributes (severity, location)  
 313 and infers the spatiotemporal scope of the impact (e.g., “Lane closure on Highway A will cause  
 314 upstream congestion propagation”).
- 315 2. **Hypothesis Verification:** The model compares the inferred impact against the statistical  
 316 properties of each candidate  $\mathcal{T}_{traj}^{(k)}$ . For instance, if the event implies a significant speed drop,  
 317 candidates showing “stable high speed” are rejected.
- 318 3. **Optimal Selection:** The index  $k^*$  corresponding to the candidate that maximizes semantic  
 319 alignment with the reasoning  $\mathcal{R}$  is selected.

320 The final output is the specific trajectory  $\hat{\mathbf{X}}^* = \hat{\mathbf{X}}^{(k^*)}$ , which represents the event-conditioned  
321 forecast.

#### 322 4.4 Stage 3: Retrieval-Augmented Decision Support

323 The objective of Stage 3 is to translate the selected mathematical forecast  $\hat{\mathbf{X}}^*$  into actionable opera-  
324 tional insights. To ensure the recommendations are professionally grounded and adhere to standard  
325 operating procedures (SOPs), we employ a Retrieval-Augmented Generation (RAG) mechanism.

##### 326 4.4.1 Historical Knowledge Retrieval

327 We construct a historical knowledge base  $\mathcal{K} = \{(c_m, a_m)\}_{m=1}^M$ , consisting of  $M$  pairs of past traffic  
328 contexts  $c_m$  (incident types, traffic states) and their corresponding expert management actions  $a_m$   
329 (e.g., signal timing adjustments, VMS activation). To retrieve relevant few-shot examples for the  
330 current situation, we utilize a dense retriever. The current context  $s$  and forecast summary  $\hat{\mathbf{X}}^*$  are  
331 concatenated into a query  $q$ . We compute the cosine similarity between the embedding of the query  
332  $\phi(q)$  and the stored context embeddings  $\phi(c_m)$ :

$$\mathcal{S}_{rel} = \{(c_m, a_m) \mid \cos(\phi(q), \phi(c_m)) > \tau\} \quad (11)$$

333 where  $\phi(\cdot)$  is a pre-trained sentence encoder and  $\tau$  is a similarity threshold. The top- $N$  most similar  
334 pairs form the reference set  $\mathcal{S}_{rel}$ , providing the LLM with implicit “operational priors.”

##### 335 4.4.2 Actionable Report Generation

336 The final generation step synthesizes the scientific prediction with operational pragmatism. The  
337 LLM acts as a conditional generator  $G$ , producing a response  $\mathbf{Y}$  composed of a situation report  
338  $\mathbf{Y}_{rep}$  and a recommendation list  $\mathbf{Y}_{rec}$ :

$$\mathbf{Y} = G(\hat{\mathbf{X}}^*, \mathcal{T}_{ctx}, \mathcal{S}_{rel}) \quad (12)$$

339 The prompt structure enforces a dual-output format:

- 340 • **Situation Report ( $\mathbf{Y}_{rep}$ )**: A concise summary for decision-makers, highlighting the selected  
341 forecast’s critical features (e.g., “Expect 15-minute delays on Corridor B starting at 08:30 due  
342 to accident clearance”).

- 343 • **Operational Recommendations ( $\mathbf{Y}_{rec}$ )**: Specific, actionable steps derived from the re-  
344 trieval examples  $\mathcal{S}_{rel}$  but adapted to the current  $\hat{\mathbf{X}}^*$  (e.g., “Implement Signal Plan 4 at Inter-  
345 section X,” “Deploy diversion signage at Exit Y”).

346 This RAG-based approach mitigates generic or hallucinated advice, ensuring that the system’s  
347 outputs are aligned with historical best practices.

348 **5 Experiments & Results**

349 To rigorously evaluate the efficacy of the Chat-ITS framework, we present a comprehensive exper-  
350imental analysis. We first detail the experimental setup—including datasets, implementation details,  
351 baselines, and metrics—in Section 5.1. Subsequently, we report the empirical results under routine  
352 traffic conditions (Section 5.2), during anomalous events (Section 5.3), and analyze the system’s  
353 explainability (Section 5.4) and component contributions (Section 5.5).

354 **5.1 Materials and Methods**

355 **5.1.1 Datasets and Preprocessing**

356 This study utilizes multiple large-scale, real-world traffic and contextual datasets collected by Amap  
357 across China, primarily focusing on Beijing for foundational model training and broader regions for  
358 event context and specific analyses. All datasets cover the period from September 2023 to May 2024,  
359 unless otherwise specified.

360 **Spatio-Temporal Traffic Data:** The core dataset for training the probabilistic foundation  
361 model consists of high-resolution traffic state information for the urban core of Beijing. Raw traffic  
362 data was aggregated onto a regular grid with a spatial resolution of  $500m \times 500m$ . This resulted  
363 in  $N = 5,797$  distinct spatial grid cells covering the main urban road network. For each cell, key  
364 traffic state variables, including traffic volume (vehicles per interval) and average speed (km/h),  
365 were computed and aggregated into 5-minute intervals. This dataset comprises approximately 1.3  
366 billion data points, providing a comprehensive representation of urban traffic dynamics much larger  
367 than many commonly used open-source benchmarks [52].

368 **Venue-Centric Traffic Data:** To specifically capture traffic patterns influenced by large-scale  
369 public events, supplementary datasets focused on major venues were compiled.

- 370 • *Aggregated Venue Flow:* Derived from location-based service data, aggregated traffic volume  
371 information was obtained for the precise geographical boundaries and surrounding buffer areas  
372 of over 300 major venues (sports stadiums, concert halls, major tourist attractions, transport  
373 hubs) across multiple cities in China. This dataset helps model event-specific demand surges  
374 and dispersion patterns.
- 375 • *Fine-Grained Venue Grid Data:* For a subset of the venues above, traffic volume was aggregated  
376 onto a finer  $100m \times 100m$  grid covering the venue. Due to the high granularity leading to  
377 sparsity, we identified and utilized data primarily from the top-20 grid cells exhibiting the  
378 highest average historical traffic volume within each venue’s defined area, focusing analysis on  
379 the most relevant micro-locations.

380 **Contextual Event Data:** Real-time and historical event information, crucial for the LLM  
381 reasoning stage (Stage 2) and evaluation during anomalies, was primarily sourced from the Amap  
382 open platform APIs and associated historical logs for the relevant periods and geographical areas.  
383 This included:

- *Structured Construction Data*: A curated dataset encompassing over 10,000 construction events on highways and major arterials. Each entry typically includes precise location information (coordinates or road segment identifiers), scheduled start and end times, number and type of lanes affected (e.g., closure, partial blockage), and nature of the work.
- *Unstructured Anomaly Reports*: Traffic incident information disseminated via Amap, originating from user reports or official traffic authority alerts. These reports typically contain a natural language description of the incident (e.g., "Accident involving two cars on Ring Road eastbound near Exit 5, blocking right lane"), an approximate location , and a timestamp. This text serves as direct input for the LLM.

**Preprocessing:** Standard preprocessing steps were applied to the traffic datasets before model training and evaluation. Missing values in the time-series data less than 5% of points were imputed using linear interpolation while others are dropped. Traffic state features (speed, volume) were normalized using Z-score normalization based on the mean and standard deviation calculated from the training portion of the primary Beijing dataset. For GNN-based baselines, the spatial graph adjacency matrix was constructed based on road network distance threshold, with edge weights typically defined by inverse distance. Unstructured text data from anomaly reports and event information was cleaned to remove irrelevant artifacts before being fed into the LLM prompts.

### 5.1.2 Baseline Implementations

The chosen baselines represent a broad spectrum of modern time series forecasting methodologies, ensuring a robust and comprehensive comparison against different architectures:

- DLinear[13]: Represents simple yet surprisingly effective linear models, serving as a strong benchmark against more complex architectures by decomposing the time series and applying separate linear layers. It challenges the necessity of intricate designs for certain forecasting tasks.
- FiLM [53]: Represents linear models enhanced with frequency analysis, designed to improve forecasting by better capturing periodicity through specific decomposition techniques applied in the frequency domain.
- Informer [54]: A prominent Transformer-based model optimized for long sequence time-series forecasting (LSTF) efficiency through a ProbSparse self-attention mechanism and distilling operation, representing efficient Transformer variants.
- PatchTST [30]: Represents channel-independent Transformer approaches utilizing patching, where input time series are divided into subseries-level patches that are fed as tokens to the Transformer, capturing local semantic information.
- Chronos [35]: Represents recent large pre-trained foundation models for time series, leveraging language model architectures scaled to time series data for zero-shot or few-shot forecasting, showcasing the potential of large-scale pre-training.

- 420     • iTransformer [31]: An innovative Transformer architecture that inverts the standard process  
 421       by applying attention to embedded variates across the entire time series length, designed to  
 422       better capture multivariate correlations.

423     For implementation, we utilized established frameworks such as TSLib [55, 56] or the official  
 424     public code repositories associated with each baseline model. To guarantee a fair and direct com-  
 425     parison, all baseline models were trained using the identical historical dataset that was employed  
 426     for training the Chat-ITS foundation model. The sole exception was Chronos, for which we lever-  
 427     aged the publicly available pre-trained weights, applying it directly as a zero-shot forecaster without  
 428     fine-tuning on our specific dataset.

429     **5.1.3 Evaluation Details**

430     We evaluated the model’s performance using standard time-series forecasting metrics: Mean Abso-  
 431     lute Error (MAE), Mean Squared Error (MSE), Root Mean Squared Error (RMSE), Mean Absolute  
 432     Percentage Error (MAPE), and Weighted Absolute Percentage Error (WAPE). MAE measures the  
 433     average absolute difference between predictions and actual values. MSE computes the average of  
 434     the squared errors, which emphasizes larger deviations more heavily. RMSE is the square root of  
 435     MSE, bringing the error back to the original scale of the data. MAPE and WAPE assess the relative  
 436     size of errors compared to actual values, providing scale-independent evaluation.

437     It is worth noting that we preferred WAPE over MAPE for traffic volume forecasting tasks, where  
 438     the data often contains zero or near-zero values. In such scenarios, MAPE can become undefined or  
 439     unstable due to division by zero or extremely small actual values, leading to misleading evaluations.  
 440     Additionally, in cases with large variance in traffic volumes, MAPE tends to overemphasize errors in  
 441     low-volume periods while underrepresenting high-volume ones. In contrast, WAPE normalizes total  
 442     absolute error by the sum of actual values across all time steps and locations, offering a more stable  
 443     and representative metric under these conditions.

444     The specific metrics are defined as (13), (14), (15), (16), and (17):

$$\text{MAE} = \frac{1}{nN} \sum_{t=T+1}^{T+n} \sum_{i=1}^N |x_{t,i} - \hat{x}_{t,i}| \quad (13)$$

$$\text{MSE} = \frac{1}{nN} \sum_{t=T+1}^{T+n} \sum_{i=1}^N (x_{t,i} - \hat{x}_{t,i})^2 \quad (14)$$

$$\text{RMSE} = \sqrt{\text{MSE}} = \sqrt{\frac{1}{nN} \sum_{t=T+1}^{T+n} \sum_{i=1}^N (x_{t,i} - \hat{x}_{t,i})^2} \quad (15)$$

$$\text{MAPE} = \frac{1}{nN} \sum_{t=T+1}^{T+n} \sum_{i=1}^N \left| \frac{x_{t,i} - \hat{x}_{t,i}}{x_{t,i}} \right| \quad (16)$$

$$\text{WAPE} = \frac{\sum_{t=T+1}^{T+n} \sum_{i=1}^N |x_{t,i} - \hat{x}_{t,i}|}{\sum_{t=T+1}^{T+n} \sum_{i=1}^N |x_{t,i}|} \quad (17)$$

449     **Anomaly Identification:** For evaluating performance during anomalies, event periods were  
 450 identified using timestamps from the Amap/Gaode construction and incident logs. Anomalous  
 451 periods were defined as 1 hour before to 1 hours after the logged event time for relevant locations.  
 452 For public events, the anomalous period covered 2 hours before the event start to 2 hours after  
 453 the event end. Zero-shot evaluation used events from categories completely held out during any  
 454 training/fine-tuning.

455     **Data Splits:** Data was split chronologically for each city/dataset. Typically, the first 70% was  
 456 used for pre-training the foundation model, the next 10% for validation, and the final 20% for testing.

## 457 5.2 Baseline Performance under Routine Conditions

458 To establish the foundational capability of our framework, we evaluated the performance of the  
 459 pre-trained spatio-temporal model (Stage 1 output) under routine traffic conditions, comparing it  
 460 against established baselines. The evaluation used Beijing datasets (Jan-May 2024), excluding major  
 461 anomalies.

462 Our results, summarized in Table 1, demonstrate that the Chat-ITS foundational model sub-  
 463 stantially outperforms all evaluated deep learning baselines under these normal conditions. Across  
 464 all prediction horizons (15, 30, and 60 minutes) and all metrics (MAE, MSE, WAPE), our model  
 465 consistently achieved the lowest error rates. Notably, while Informer emerged as the most com-  
 466 petitive baseline, our model still surpassed its performance considerably. For instance, the average  
 467 MAE for our model (0.153) was markedly lower than Informer’s (0.166) and substantially better  
 468 than PatchTST (0.259) or FiLM (0.527).

469 Furthermore, our model displayed remarkable stability across prediction horizons, maintaining  
 470 consistently low error values even for 60-minute forecasts. This contrasts with baselines like DLin-  
 471 ear and PatchTST, which exhibited pronounced accuracy degradation as the horizon increased.  
 472 This confirms that the foundation model provides a robust starting point for subsequent contextual  
 473 adjustment.

Table 1: Comparison of forecasting metrics (MAE, MSE and WAPE) under routine traffic conditions for different prediction horizons (15, 30, 60 min, and average). Models compared include our pre-trained spatio-temporal model and selected deep learning baselines (e.g., DLinear, FiLM, Informer, PatchTST, Chronos, iTransformer) on the Beijing dataset. Best results for each metric and horizon are highlighted.

	15 min			30 min			60 min			Average	
	MAE	MSE	WAPE	MAE	MSE	WAPE	MAE	MSE	WAPE	MAE	WAPE
DLinear	0.270	0.139	0.384	0.374	0.257	0.532	0.542	0.508	0.769	0.383	0.285
FiLM	0.423	0.301	0.602	0.534	0.491	0.759	0.669	0.772	0.949	0.527	0.496
Informer	0.161	0.060	0.229	0.167	0.066	0.237	0.176	0.074	0.249	0.166	0.066
PatchTST	0.201	0.090	0.286	0.251	0.147	0.356	0.347	0.285	0.491	0.259	0.164
chronos-b	0.423	0.427	0.561	0.342	0.323	0.495	0.291	0.325	0.425	0.424	0.489
chronos-m	0.433	0.426	0.574	0.351	0.328	0.508	0.301	0.343	0.440	0.431	0.495
chronos-s	0.439	0.443	0.582	0.349	0.325	0.505	0.311	0.374	0.454	0.436	0.504
iTransformer	0.194	0.088	0.275	0.226	0.130	0.321	0.293	0.234	0.416	0.233	0.143
<b>Ours</b>	<b>0.153</b>	<b>0.055</b>	<b>0.217</b>	<b>0.151</b>	<b>0.054</b>	<b>0.215</b>	<b>0.158</b>	<b>0.058</b>	<b>0.225</b>	<b>0.153</b>	<b>0.055</b>
											<b>0.217</b>

### 474 5.3 Enhanced Prediction Accuracy across Diverse Anomalous Events

475 We assessed the core contribution of Chat-ITS—integrating contextual information via LLM—using  
 476 two distinct datasets: scheduled highway construction projects and unplanned traffic incidents. We  
 477 compared the final Chat-ITS forecasts against a **Zero-shot** baseline (foundation model only) and a  
 478 **Few-shot/Fine-tuned** baseline (foundation model fine-tuned on anomaly data).

479 As shown in Table 2, Chat-ITS demonstrated superior prediction accuracy compared to both  
 480 baselines across all horizons. Compared to the Zero-shot forecast, Chat-ITS consistently reduced  
 481 prediction errors (e.g., lower MAE). Crucially, Chat-ITS also outperformed the Fine-tuned strategy.  
 482 This suggests that the LLM’s ability to reason from explicit, real-time contextual descriptions (like  
 483 construction schedules) is a more potent adaptation mechanism than relying solely on learning from  
 484 limited historical patterns of disruptions.

485 Figure 2 provides illustrative examples. In a construction scenario (Figure 2a), the foundation  
 486 model underestimated the disruption severity. However, Chat-ITS, processing the text ”one lane  
 487 closed for 4 hours,” inferred the non-linear impact on capacity and correctly predicted a sharp drop  
 488 in speed and sustained low volume, aligning with ground truth. In an incident scenario (Figure  
 489 2b), the foundation model assumed a quick recovery. In contrast, the LLM reasoned that the ”full  
 490 closure” and ”diversion to bypass” would cause a severe, prolonged speed drop, yielding a forecast  
 491 that closely tracked the observed traffic collapse. These results highlight how embedding domain-  
 492 specific reasoning bridges the gap between statistical forecasting and operational reality.

Table 2: Forecasting accuracy improvements during anomalous events. Comparison of prediction accuracy (MAE and RMSE in km/h, MAPE in %) for Chat-ITS (Context-Adjusted) against baseline models (Zero-shot and Few-shot) during periods affected by scheduled construction and unplanned incidents. Data evaluated on the anomaly datasets across different prediction horizons. Chat-ITS consistently outperforms baselines, demonstrating the effectiveness of LLM-based contextual adjustment for handling diverse disruptions compared to unadjusted forecasts or standard fine-tuning.

	15 min				30 min				60 min				Average	
	MAE	RMSE	MAPE	MAE	RMSE	MAPE	MAE	RMSE	MAPE	MAE	RMSE	MAPE	RMSE	MAPE
<b>Few-shot</b>	5.11	8.25	18.11%	5.63	9.27	21.18%	6.36	10.57	23.56%	5.59	9.25	20.59%		
<b>Zero-shot</b>	5.19	8.33	18.71%	5.69	9.33	21.69%	6.47	10.72	25.90%	5.67	9.34	21.38%		
<b>Chat-ITS</b>	<b>4.86</b>	<b>8.03</b>	<b>16.51%</b>	<b>5.31</b>	<b>8.98</b>	<b>18.45%</b>	<b>5.94</b>	<b>10.19</b>	<b>20.58%</b>	<b>5.27</b>	<b>8.97</b>	<b>18.18%</b>		

### 493 5.4 Explainable Reporting and Actionable Recommendations

494 Stage 3 of the framework utilizes the LLM to translate quantitative forecasts into human-readable  
 495 reports. Figure 3 showcases this capability:

- 496 • **Routine Scenario:** The LLM provides concise confirmation (”Expect typical heavy conges-  
 497 tion”) and prompts standard checks (”Ensure ramp metering active”), building trust.
- 498 • **Construction Event:** The output is analytical, synthesizing the speed drop with the ”single  
 499 lane closure” context. Recommendations are proactive, suggesting ”deploying VMS advisory”

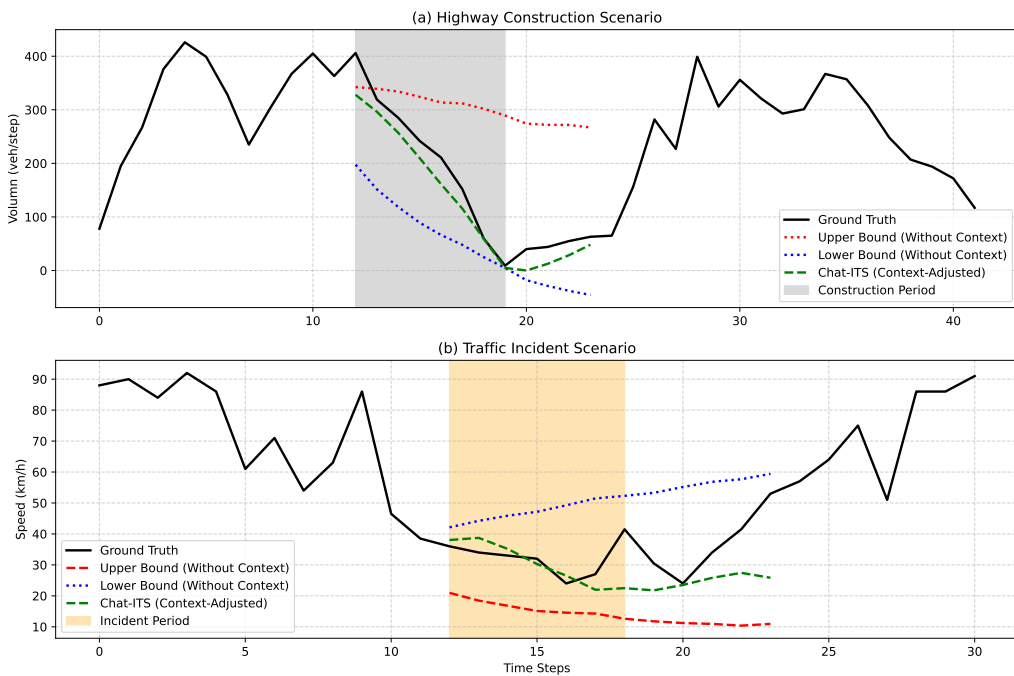


**Figure 2: Chat-ITS enhances forecasting accuracy during anomalous events.** Time-series comparison of predicted traffic states versus ground truth. **(a)**, Highway construction scenario. **(b)**, Traffic incident scenario. The green dashed line (Chat-ITS) tracks the ground truth (black solid) more accurately than the foundation model baselines (red/blue dotted) by incorporating event context.

## LLM-generated Explainable Reports and Actionable Recommendations

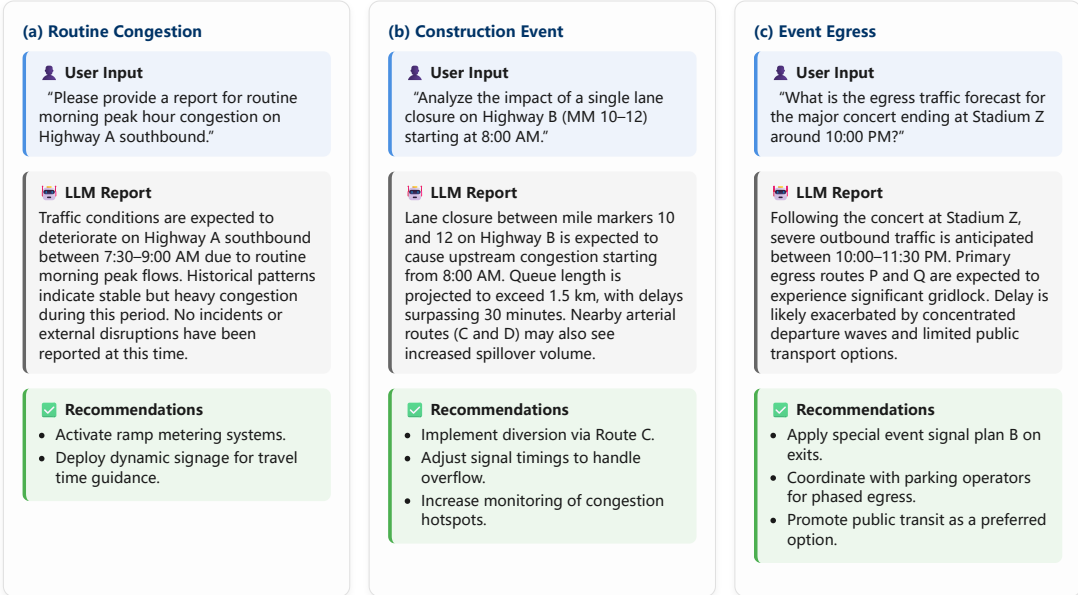


Figure 3: **LLM-generated explainable reports and actionable recommendations.** Examples regarding (a) Routine Congestion, (b) Construction Event, and (c) Public Event Egress, showing the translation from context-aware prediction to operational intelligence.

500 and "adjusting signal timings" on alternate routes, demonstrating reasoning about network-wide ripple effects.  
501

502 • **Public Event:** The report highlights specific egress congestion timing. Recommendations  
503 like "Monitor parking lot clearance rates" are highly tailored to the event type.

504 These outputs demonstrate Chat-ITS's capacity to bridge the gap between prediction and action,  
505 transforming numerical data into operationally relevant intelligence.

### 506 5.5 Ablation Studies

507 We performed ablation studies on the anomaly dataset to validate component contributions:

- 508 1. **Necessity of LLM Adjustment:** Removing Stage 2 and relying solely on the foundation  
509 model resulted in noticeable accuracy degradation during anomalies (Figure 4a), confirming  
510 the essential role of contextual reasoning.
- 511 2. **Probabilistic vs. Deterministic Input:** Providing the LLM with multiple probabilistic  
512 candidate trajectories (Stage 1 output) yielded better performance than providing a single

Ablation Study on Chat-ITS Variants

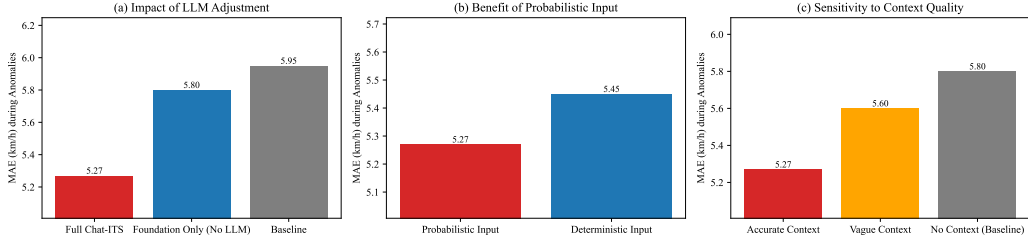


Figure 4: **Ablation study results.** (a) Impact of removing LLM adjustment. (b) Benefit of probabilistic candidates vs. deterministic input. (c) Sensitivity to context quality.

513 deterministic mean forecast (Figure 4b). This suggests the probabilistic distribution offers a  
514 richer search space for the LLM to select the most contextually plausible outcome.

515 **3. Context Quality:** While performance dropped when input context was intentionally de-  
516 graded (vague/incorrect), Chat-ITS still outperformed context-unaware baselines, indicating  
517 a degree of robustness (Figure 4c).

## 518 6 Discussion

519 In this work, we introduced Chat-ITS, a hybrid framework that synergistically combines a pre-  
520 trained spatio-temporal foundation model for probabilistic forecasting with the contextual reasoning  
521 capabilities of Large Language Models to address key limitations in current traffic prediction systems.  
522 Our results demonstrate that Chat-ITS achieves forecasting accuracy comparable to state-of-the-art  
523 deep learning methods under routine traffic conditions. More importantly, it marked outperforms  
524 these baselines during anomalous events, such as construction, incidents, and public gatherings,  
525 by effectively incorporating real-time structured and unstructured contextual information via LLM  
526 processing. We showed substantial error reductions (up to 15%) during such events, highlighting the  
527 framework’s enhanced adaptability and resilience. Furthermore, case studies illustrated Chat-ITS’s  
528 promising zero-shot generalization capability, allowing it to interpret and respond to novel event  
529 types described solely through natural language prompts. Finally, we demonstrated the framework’s  
530 ability to generate explainable, human-readable summary reports and actionable traffic management  
531 recommendations, bridging the critical gap between prediction and operational decision-making.

532 The effectiveness of Chat-ITS stems from its deliberate hybrid design, which leverages the com-  
533plementary strengths of deep learning for pattern recognition in high-dimensional spatio-temporal  
534 data and LLMs for flexible context understanding, reasoning, and natural language generation. The  
535 foundation model provides a statistically robust baseline forecast capturing complex recurring dy-  
536 namics and uncertainty. The LLM, instead of being burdened with direct numerical prediction,  
537 focuses on its core strengths: interpreting diverse inputs (text, structured data), inferring causal im-  
538 pacts of events, evaluating scenarios based on context, and communicating findings effectively. This  
539 division of labor allows Chat-ITS to overcome the brittleness of purely data-driven models during

540 anomalies and the limitations of purely LLM-based approaches in precise numerical forecasting. The  
541 integration of historical dispatch patterns further enhances the practical relevance of the generated  
542 recommendations. This synergistic approach represents a noticeable step towards ITS that are not  
543 only predictive but also adaptive, explainable, and operationally relevant.

544 The uniqueness of Chat-ITS lies in its synergistic integration of two powerful AI paradigms:  
545 deep learning for robust forecasting and LLMs for contextual reasoning. While deep learning mod-  
546 els have pushed the boundaries of accuracy on benchmark datasets, they often lack robustness to  
547 out-of-distribution events and fail to provide actionable insights. Attempts to incorporate auxiliary  
548 data often rely on rigid input structures and struggle with unstructured text. LLM applications in  
549 transportation have primarily focused on tasks like route planning, dialogue systems, or summarizing  
550 traffic reports, but their direct application to end-to-end numerical forecasting remains challenging.  
551 Chat-ITS uniquely integrates these two powerful AI paradigms in a way that mitigates their re-  
552 spective weaknesses while harnessing their combined potential for context-aware, explainable, and  
553 actionable traffic prediction.

554 The performance of Chat-ITS during anomalies is inherently dependent on the availability and  
555 quality of real-time contextual information ( $\mathbf{s}$ ). Inaccurate or delayed event reports will naturally  
556 limit the effectiveness of the LLM adjustment stage. While we demonstrated some robustness,  
557 further research is needed on handling noisy or conflicting contextual inputs. The reliance on LLMs  
558 also introduces computational costs associated with inference, although using smaller or optimized  
559 LLMs could mitigate this, and exploring different LLM architectures, including potentially smaller,  
560 domain-adapted models, could optimize this trade-off. Potential issues related to LLM biases or  
561 hallucinations, while mitigated by grounding the LLM’s task in evaluating pre-generated trajectories,  
562 require ongoing vigilance and potentially safety layers in operational deployment. Furthermore,  
563 effective prompt engineering is crucial for eliciting the desired reasoning and output from the LLM,  
564 which may require domain expertise. Scalability to extremely large, city-wide networks with tens of  
565 thousands of sensors also needs further investigation.

566 Future research will focus on integrating Chat-ITS with real-time traffic control systems (e.g.,  
567 adaptive signal control, variable speed limits) to enable fully automated, context-aware traffic man-  
568 agement. We also aim to incorporate a wider range of contextual data sources, such as real-time  
569 social media feeds, advanced weather nowcasting, or connected vehicle data, to further enhance  
570 situational awareness. Developing more sophisticated methods for the LLM to not just select but  
571 actively modify forecast trajectories based on context could yield further accuracy gains. Finally,  
572 conducting user studies with traffic operators to evaluate the usability and effectiveness of the gen-  
573 erated reports and recommendations in real-world control room settings is essential for practical  
574 validation and refinement.

## 575 Acknowledgments

576 This work was supported by Beijing Natural Science Foundation (No. JQ24051), Beijing Nova  
577 Program (No. 20230484432) and Independent Research Project of the State Key Laboratory of  
578 Intelligent Green Vehicle and Mobility, Tsinghua University (No. ZZ-GG-20250406).

579    **7 Data Availability**

580    The datasets central to this study, including the large-scale traffic network data and the anomalous  
581    event logs, were provided by Amap. Due to the proprietary nature of this information, which encom-  
582    passes commercial sensitivities and privacy considerations, these datasets are not publicly available.  
583    We acknowledge the importance of reproducibility and regret that these necessary restrictions pre-  
584    vent the public dissemination of these materials. Enquiries regarding the methodology or potential  
585    collaborations may be directed to the corresponding author.

586    **8 Supplementary Materials**

- 587    • **Text S1 and Table S1.** Detailed description and illustrative examples of the Structured  
588    Construction Data used in this study.
- 589    • **Text S2 and Table S2.** Detailed description and examples of the Unstructured Anomaly  
590    Reports.

591    **References**

- 592    1. Wu K, Ding J, Lin J, et al. Big-data empowered traffic signal control could reduce urban carbon  
593    emission. *Nature Communications* 2025;16. Publisher: Nature Publishing Group:2013.
- 594    2. Avila AM and Mezić I. Data-driven analysis and forecasting of highway traffic dynamics. *Nature  
595    Communications* 2020;11. Publisher: Nature Publishing Group TLDR: Here it is demonstrated  
596    how the Koopman mode decomposition can offer a model-free, data-driven approach for ana-  
597    lyzing and forecasting traffic dynamics.:2090.
- 598    3. Shao Z, Zhang Z, Wang F, and Xu Y. Pre-training Enhanced Spatial-temporal Graph Neural  
599    Network for Multivariate Time Series Forecasting. In: *Proceedings of the 28th ACM SIGKDD  
600    Conference on Knowledge Discovery and Data Mining*. 2022:1567–77. DOI: 10.1145/3534678.  
601    3539396. arXiv: 2206 . 09113[cs]. URL: <http://arxiv.org/abs/2206.09113> (visited on  
602    10/24/2023).
- 603    4. Li Z, Cai R, Fu TZJ, Hao Z, and Zhang K. Transferable Time-Series Forecasting Under Causal  
604    Conditional Shift. *IEEE Transactions on Pattern Analysis and Machine Intelligence* 2024;46.  
605    Conference Name: IEEE Transactions on Pattern Analysis and Machine Intelligence:1932–49.
- 606    5. Runge J, Bathiany S, Boltt E, et al. Inferring causation from time series in Earth system  
607    sciences. *Nature Communications* 2019;10. Publisher: Nature Publishing Group:2553.
- 608    6. Yuan Y, Ding J, Feng J, Jin D, and Li Y. UniST: A Prompt-Empowered Universal Model  
609    for Urban Spatio-Temporal Prediction. 2024. DOI: 10.1145/3637528.3671662. arXiv: 2402.  
610    11838[cs]. URL: <http://arxiv.org/abs/2402.11838> (visited on 07/15/2024).

- 611 7. Guo X, Zhang Q, Jiang J, Peng M, Zhu M, and Yang HF. Towards explainable traffic flow  
612 prediction with large language models. Communications in Transportation Research 2024;4.  
613 TLDR: This paper proposes a Traffic flow Prediction model based on Large Language Models  
614 (LLMs) to generate explainable traffic predictions, named xTP-LLM, and is the first study to  
615 use LLM for explainable prediction of traffic flows.:100150.
- 616 8. Williams AR, Ashok A, Marcotte É, et al. Context is Key: A Benchmark for Forecasting  
617 with Essential Textual Information. TLDR: A time series forecasting benchmark that pairs  
618 numerical data with diverse types of carefully crafted textual context, requiring models to  
619 integrate both modalities, and a simple yet effective LLM prompting method that outperforms  
620 all other tested methods on this benchmark. 2024. DOI: 10.48550/arXiv.2410.18959. arXiv:  
621 2410.18959[cs]. URL: <http://arxiv.org/abs/2410.18959> (visited on 01/08/2025).
- 622 9. Liu H, Xu S, Zhao Z, et al. Time-MMD: A New Multi-Domain Multimodal Dataset for Time  
623 Series Analysis. TLDR: Time-MMD is introduced, the first multi-domain, multimodal time  
624 series dataset covering 9 primary data domains, and MM-TSFLib, the first multimodal time-  
625 series forecasting (TSF) library, seamlessly pipelining multimodal TSF evaluations based on  
626 Time-MMD for in-depth analyses. 2024. DOI: 10.48550/arXiv.2406.08627. arXiv: 2406.  
627 08627[cs]. URL: <http://arxiv.org/abs/2406.08627> (visited on 07/26/2024).
- 628 10. Li Z, Lin X, Liu Z, et al. Language in the Flow of Time: Time-Series-Paired Texts Weaved  
629 into a Unified Temporal Narrative. 2025. DOI: 10.48550/arXiv.2502.08942. arXiv: 2502.  
630 08942[cs]. URL: <http://arxiv.org/abs/2502.08942> (visited on 02/17/2025).
- 631 11. Xue H and Salim FD. PromptCast: A New Prompt-based Learning Paradigm for Time Series  
632 Forecasting. 2023. DOI: 10.48550/arXiv.2210.08964. arXiv: 2210.08964[cs, math, stat].  
633 URL: <http://arxiv.org/abs/2210.08964> (visited on 01/17/2024).
- 634 12. Arango SP, Mercado P, Kapoor S, et al. ChronosX: Adapting Pretrained Time Series Mod-  
635 els with Exogenous Variables. TLDR: This paper introduces a new method to incorporate  
636 covariates into pretrained time series forecasting models through modular blocks that inject  
637 past and future covariate information, without necessarily modifying the pretrained model  
638 in consideration. 2025. DOI: 10.48550/arXiv.2503.12107. arXiv: 2503.12107[cs]. URL:  
639 <http://arxiv.org/abs/2503.12107> (visited on 03/27/2025).
- 640 13. Zeng A, Chen M, Zhang L, and Xu Q. Are Transformers Effective for Time Series Forecast-  
641 ing? 2022. arXiv: 2205.13504[cs]. URL: <http://arxiv.org/abs/2205.13504> (visited on  
642 07/25/2023).
- 643 14. Tan M, Merrill MA, Gupta V, Althoff T, and Hartvigsen T. Are Language Models Actually  
644 Useful for Time Series Forecasting? 2024. DOI: 10.48550/arXiv.2406.16964. arXiv: 2406.  
645 16964[cs]. URL: <http://arxiv.org/abs/2406.16964> (visited on 08/06/2024).
- 646 15. Yuan X and Qiao Y. Diffusion-TS: Interpretable Diffusion for General Time Series Generation.  
647 In: The Twelfth International Conference on Learning Representations. 2023. URL: <https://openreview.net/forum?id=4h1apFj099> (visited on 12/13/2024).

- 649 16. Su J, Jiang C, Jin X, et al. Large Language Models for Forecasting and Anomaly Detection:  
650 A Systematic Literature Review. 2024. DOI: 10.48550/arXiv.2402.10350. arXiv: 2402.  
651 10350[cs]. URL: <http://arxiv.org/abs/2402.10350> (visited on 04/02/2024).
- 652 17. Wang X, Fang M, Zeng Z, and Cheng T. Where Would I Go Next? Large Language Models  
653 as Human Mobility Predictors. 2023. DOI: 10.48550/arXiv.2308.15197. arXiv: 2308.  
654 15197[physics]. URL: <http://arxiv.org/abs/2308.15197> (visited on 10/30/2023).
- 655 18. Feng J, Du Y, Liu T, Guo S, Lin Y, and Li Y. CityGPT: Empowering Urban Spatial Cognition  
656 of Large Language Models. 2024. DOI: 10.48550/arXiv.2406.13948. arXiv: 2406.13948[cs].  
657 URL: <http://arxiv.org/abs/2406.13948> (visited on 08/01/2024).
- 658 19. Liu P, Guo H, Dai T, et al. Taming Pre-trained LLMs for Generalised Time Series Forecasting  
659 via Cross-modal Knowledge Distillation. 2024. DOI: 10.48550/arXiv.2403.07300. arXiv:  
660 2403.07300[cs]. URL: <http://arxiv.org/abs/2403.07300> (visited on 03/19/2024).
- 661 20. Jin M, Wang S, Ma L, et al. Time-LLM: Time Series Forecasting by Reprogramming Large  
662 Language Models. 2023. DOI: 10.48550/arXiv.2310.01728. arXiv: 2310.01728[cs]. URL:  
663 <http://arxiv.org/abs/2310.01728> (visited on 10/19/2023).
- 664 21. Ma X, Tao Z, Wang Y, Yu H, and Wang Y. Long short-term memory neural network for  
665 traffic speed prediction using remote microwave sensor data. Transportation Research Part C:  
666 Emerging Technologies 2015;54. Publisher: Elsevier:187–97.
- 667 22. Ma X, Zhong H, Li Y, Ma J, Cui Z, and Wang Y. Forecasting Transportation Network Speed  
668 Using Deep Capsule Networks With Nested LSTM Models. IEEE Transactions on Intelligent  
669 Transportation Systems 2021;22. Conference Name: IEEE Transactions on Intelligent Trans-  
670 portation Systems:4813–24.
- 671 23. Li Y, Yu R, Shahabi C, and Liu Y. Diffusion convolutional recurrent neural network: Data-  
672 driven traffic forecasting. arXiv preprint arXiv:1707.01926 2017.
- 673 24. Wu Z, Pan S, Long G, Jiang J, and Zhang C. Graph wavenet for deep spatial-temporal graph  
674 modeling. arXiv preprint arXiv:1906.00121 2019.
- 675 25. Yan H, Ma X, and Pu Z. Learning Dynamic and Hierarchical Traffic Spatiotemporal Features  
676 With Transformer. IEEE Transactions on Intelligent Transportation Systems 2022;23. Confer-  
677 ence Name: IEEE Transactions on Intelligent Transportation Systems:22386–99.
- 678 26. Jiang J, Han C, Zhao WX, and Wang J. PDFormer: Propagation Delay-Aware Dynamic Long-  
679 Range Transformer for Traffic Flow Prediction. 2023. DOI: 10.48550/arXiv.2301.07945.  
680 arXiv: 2301.07945[cs]. URL: <http://arxiv.org/abs/2301.07945> (visited on 02/06/2024).
- 681 27. Liu X, Liang Y, Huang C, et al. Do We Really Need Graph Neural Networks for Traffic  
682 Forecasting? TLDR: Empirical results show that SimST improves the prediction throughput  
683 by up to 39 times compared to more sophisticated STGNNs while attaining comparable per-  
684 formance, which indicates that GNNs are not the only option for spatial modeling in traffic  
685 forecasting. 2023. DOI: 10.48550/arXiv.2301.12603. arXiv: 2301.12603[cs]. URL: <http://arxiv.org/abs/2301.12603> (visited on 01/05/2024).

- 687 28. Wang Z, Nie Y, Sun P, Nguyen NH, Mulvey J, and Poor HV. ST-MLP: A Cascaded Spatio-  
688 Temporal Linear Framework with Channel-Independence Strategy for Traffic Forecasting. 2023.  
689 DOI: 10.48550/arXiv.2308.07496. arXiv: 2308.07496[cs]. URL: <http://arxiv.org/abs/2308.07496> (visited on 01/05/2024).
- 690  
691 29. Shao Z, Zhang Z, Wang F, Wei W, and Xu Y. Spatial-Temporal Identity: A Simple yet Effective  
692 Baseline for Multivariate Time Series Forecasting. 2022. DOI: 10.48550/arXiv.2208.05233.  
693 arXiv: 2208.05233[cs]. URL: <http://arxiv.org/abs/2208.05233> (visited on 01/08/2024).
- 694  
695 30. Nie Y, Nguyen NH, Sinthong P, and Kalagnanam J. A Time Series is Worth 64 Words: Long-  
696 term Forecasting with Transformers. 2023. arXiv: 2211.14730[cs]. URL: <http://arxiv.org/abs/2211.14730> (visited on 12/15/2023).
- 697  
698 31. Liu Y, Hu T, Zhang H, et al. iTransformer: Inverted Transformers Are Effective for Time  
699 Series Forecasting. 2023. DOI: 10.48550/arXiv.2310.06625. arXiv: 2310.06625[cs]. URL:  
700 <http://arxiv.org/abs/2310.06625> (visited on 10/24/2023).
- 701  
702 32. Lin L, Shi D, Han A, and Gao J. SpecSTG: A Fast Spectral Diffusion Framework for Probabilistic  
703 Spatio-Temporal Traffic Forecasting. 2024. DOI: 10.48550/arXiv.2401.08119. arXiv:  
704 2401.08119[cs]. URL: <http://arxiv.org/abs/2401.08119> (visited on 05/09/2024).
- 705  
706 33. Liang Y, Wen H, Nie Y, et al. Foundation Models for Time Series Analysis: A Tutorial and  
707 Survey. 2024. DOI: 10.48550/arXiv.2403.14735. arXiv: 2403.14735[cs]. URL: <http://arxiv.org/abs/2403.14735> (visited on 05/07/2024).
- 708  
709 34. Jin M, Wen Q, Liang Y, et al. Large Models for Time Series and Spatio-Temporal Data: A  
710 Survey and Outlook. 2023. DOI: 10.48550/arXiv.2310.10196. arXiv: 2310.10196[cs]. URL:  
711 <http://arxiv.org/abs/2310.10196> (visited on 10/25/2023).
- 712  
713 35. Ansari AF, Stella L, Turkmen C, et al. Chronos: Learning the Language of Time Series. 2024.  
714 arXiv: 2403.07815[cs]. URL: <http://arxiv.org/abs/2403.07815> (visited on 03/18/2024).
- 715  
716 36. Rasul K, Ashok A, Williams AR, et al. Lag-Llama: Towards Foundation Models for Time  
717 Series Forecasting. 2023. DOI: 10.48550/arXiv.2310.08278. arXiv: 2310.08278[cs]. URL:  
718 <http://arxiv.org/abs/2310.08278> (visited on 10/18/2023).
- 719  
720 37. Wu H, Hu T, Liu Y, Zhou H, Wang J, and Long M. TIMESNET: TEMPORAL 2D-VARIATION  
721 MODELING FOR GENERAL TIME SERIES ANALYSIS. 2023.
- 722  
723 38. Gao S, Koker T, Queen O, Hartvigsen T, Tsilgkaridis T, and Zitnik M. UniTS: Building a  
724 Unified Time Series Model. 2024. arXiv: 2403.00131[cs]. URL: <http://arxiv.org/abs/2403.00131> (visited on 03/18/2024).
- 725  
726 39. Liu X, Liu J, Woo G, et al. Moirai-MoE: Empowering Time Series Foundation Models with  
727 Sparse Mixture of Experts. 2024. DOI: 10.48550/arXiv.2410.10469. arXiv: 2410.10469. URL:  
728 <http://arxiv.org/abs/2410.10469> (visited on 11/12/2024).
- 729  
730 40. Zhou T, Niu P, Wang X, Sun L, and Jin R. One Fits All: Power General Time Series Analysis  
731 by Pretrained LM. 2023. arXiv: 2302.11939[cs]. URL: <http://arxiv.org/abs/2302.11939>  
732 (visited on 10/18/2023).

- 725 41. Jin M, Tang H, Zhang C, et al. Time Series Forecasting with LLMs: Understanding and En-  
726 hancing Model Capabilities. arXiv.org. 2024. URL: <https://arxiv.org/abs/2402.10835v2>  
727 (visited on 05/07/2024).
- 728 42. Chang C, Peng WC, and Chen TF. LLM4TS: Two-Stage Fine-Tuning for Time-Series Forecast-  
729 ing with Pre-Trained LLMs. 2023. DOI: 10.48550/arXiv.2308.08469. arXiv: 2308.08469[cs].  
730 URL: <http://arxiv.org/abs/2308.08469> (visited on 10/19/2023).
- 731 43. Li Z, Xia L, Tang J, et al. UrbanGPT: Spatio-Temporal Large Language Models. 2024. DOI:  
732 10.48550/arXiv.2403.00813. arXiv: 2403.00813[cs]. URL: <http://arxiv.org/abs/2403.00813>  
733 (visited on 03/21/2024).
- 734 44. Liu C, Yang S, Xu Q, et al. Spatial-Temporal Large Language Model for Traffic Prediction.  
735 2024. DOI: 10.48550/arXiv.2401.10134. arXiv: 2401.10134[cs]. URL: <http://arxiv.org/abs/2401.10134>  
736 (visited on 01/22/2024).
- 737 45. Guo X, Zhang Q, Peng M, Zhu M, Hao, and Yang. Explainable Traffic Flow Prediction with  
738 Large Language Models. version: 2. 2024. arXiv: 2404.02937[cs]. URL: <http://arxiv.org/abs/2404.02937>  
739 (visited on 04/09/2024).
- 740 46. Zhang C, Zhang Y, Shao Q, et al. ChatTraffic: Text-to-Traffic Generation via Diffusion Model.  
741 2024. DOI: 10.48550/arXiv.2311.16203. arXiv: 2311.16203[cs]. URL: <http://arxiv.org/abs/2311.16203>  
742 (visited on 12/19/2024).
- 743 47. Lee G, Yu W, Shin K, Cheng W, and Chen H. TimeCAP: Learning to Contextualize, Augment,  
744 and Predict Time Series Events with Large Language Model Agents. TLDR: Experimental  
745 results on real-world datasets demonstrate that TimeCAP outperforms state-of-the-art methods  
746 for time series event prediction, including those utilizing LLMs as predictors, achieving an  
747 average improvement of 28.75% in F1 score. 2025. DOI: 10.48550/arXiv.2502.11418. arXiv:  
748 2502.11418[cs]. URL: <http://arxiv.org/abs/2502.11418> (visited on 03/18/2025).
- 749 48. Jiang Y, Yu W, Lee G, et al. Explainable Multi-modal Time Series Prediction with LLM-in-the-  
750 Loop. TLDR: TimeXL, a multi-modal prediction framework that integrates a prototype-based  
751 time series encoder with three collaborating Large Language Models to deliver more accurate  
752 predictions and interpretable explanations, is introduced. 2025. DOI: 10.48550/arXiv.2503.  
753 01013. arXiv: 2503.01013[cs]. URL: <http://arxiv.org/abs/2503.01013> (visited on  
754 03/12/2025).
- 755 49. Wang X, Feng M, Qiu J, Gu J, and Zhao J. From News to Forecast: Integrating Event Analysis  
756 in LLM-Based Time Series Forecasting with Reflection. TLDR: This paper utilizes LLM-based  
757 agents to iteratively filter out irrelevant news and employ human-like reasoning to evaluate pre-  
758 dictions, which enables the model to analyze complex events, such as unexpected incidents and  
759 shifts in social behavior. 2024. DOI: 10.48550/arXiv.2409.17515. arXiv: 2409.17515[cs].  
760 URL: <http://arxiv.org/abs/2409.17515> (visited on 02/28/2025).
- 761 50. Raffel C, Shazeer N, Roberts A, et al. Exploring the limits of transfer learning with a unified  
762 text-to-text transformer. Journal of machine learning research 2020;21:1–67.
- 763 51. Bai J, Bai S, Chu Y, et al. Qwen Technical Report. arXiv preprint arXiv:2309.16609 2023.

- 764 52. Liu X, Xia Y, Liang Y, et al. LargeST: A Benchmark Dataset for Large-Scale Traffic Fore-  
765 casting. 2023. arXiv: 2306.08259[cs]. URL: <http://arxiv.org/abs/2306.08259> (visited on  
766 10/31/2023).
- 767 53. Zhou T, Ma Z, Wen Q, et al. Film: Frequency improved legendre memory model for long-term  
768 time series forecasting. Advances in neural information processing systems 2022;35:12677–90.
- 769 54. Zhou H, Zhang S, Peng J, et al. Informer: Beyond efficient transformer for long sequence time-  
770 series forecasting. In: *Proceedings of the AAAI conference on artificial intelligence*. Vol. 35. 12.  
771 2021:11106–15.
- 772 55. Wu H, Hu T, Liu Y, Zhou H, Wang J, and Long M. TimesNet: Temporal 2D-Variation Modeling  
773 for General Time Series Analysis. In: *International Conference on Learning Representations*.  
774 2023.
- 775 56. Wang Y, Wu H, Dong J, Liu Y, Long M, and Wang J. Deep Time Series Models: A Compre-  
776 hensive Survey and Benchmark. 2024.